
Zeroth-Order Actor-Critic

Yuheng Lei¹ Jinayu Chen² Shengbo Eben Li¹ Sifa Zheng¹

Abstract

Zeroth-order optimization methods and policy gradient based first-order methods are two promising alternatives to solve reinforcement learning (RL) problems with complementary advantages. The former work with arbitrary policies, drive state-dependent and temporally-extended exploration, possess robustness-seeking property, but suffer from high sample complexity, while the latter are more sample efficient but restricted to differentiable policies and the learned policies are less robust. We propose Zeroth-Order Actor-Critic algorithm (ZOAC) that unifies these two methods into an on-policy actor-critic architecture to preserve the advantages from both. ZOAC conducts rollouts collection with timestep-wise perturbation in parameter space, first-order policy evaluation (PEV) and zeroth-order policy improvement (PIM) alternately in each iteration. We evaluate our proposed method on a range of challenging continuous control benchmarks using different types of policies, where ZOAC outperforms zeroth-order and first-order baseline algorithms.

1. Introduction

Reinforcement learning (RL) has achieved great success in a wide range of challenging domains, including video games (Mnih et al., 2015), robotic control (Schulman et al., 2017), autonomous driving (Kendall et al., 2019), etc. The majority of RL methods formulate the environment as Markov decision process (MDP) and leverage the temporal structure to design learning algorithms such as Q-learning and policy gradient (Sutton & Barto, 2018). Actor-critic methods are among the most popular RL algorithms, which usually introduce two function approximators, one for value function estimation (critic) and another for optimal policy approximation (actor), and optimize these two approximators by alternating between policy evaluation (PEV) and

policy improvement (PIM). On-policy actor-critic methods, e.g., A3C (Mnih et al., 2016) and PPO (Schulman et al., 2017), often use critics to construct advantage functions and substitute them for the Monte Carlo return used in vanilla policy gradient (Williams, 1992), which significantly reduces the variance of gradient estimation and improve learning speed and stability. Among existing actor-critic algorithms, a common choice is to use deep neural networks as the function approximators and conduct both PEV and PIM using first-order optimization techniques.

An alternative approach for RL, though less popular, is to ignore the underlying MDP structures and regard RL problems as black-box optimization, and to directly search for the optimal policy in a zeroth-order way, i.e., without using the first-order gradient information. Recent researches have shown that zeroth-order optimization (ZOO) methods, e.g., ES (Salimans et al., 2017), ARS (Mania et al., 2018) and GA (Such et al., 2017; Risi & Stanley, 2019), are competitive on common RL benchmarks, even when applied to deep neural network with millions of parameters or with complex heterogeneous architectures like world models (Ha & Schmidhuber, 2018). ZOO has several advantages compared to first-order MDP-based RL methods (Sehnke et al., 2010; Such et al., 2017; Lehman et al., 2018; Khadka & Tumer, 2018; Qian & Yu, 2021): (1) ZOO is not restricted to differentiable policies; (2) ZOO perturbs the policy in parameter space rather than in action space, which leads to state-dependent and temporally-extended exploration; (3) Zeroth-order population-based optimization possesses robustness-seeking property and diverse policy behaviors.

Despite these attractive advantages, the main limitation of ZOO is its high sample complexity and high variance of the parameter update process, especially in high-dimensional problems. Recent researches have proposed various techniques to improve ZOO, e.g., using orthogonal or antithetic sampling methods (Sehnke et al., 2010; Salimans et al., 2017; Choromanski et al., 2018; Mania et al., 2018), identifying a low-dimensional search subspace (Maheswaranathan et al., 2019; Choromanski et al., 2019; Sener & Koltun, 2020), or subtracting a baseline for variance reduction (Sehnke et al., 2010; Grathwohl et al., 2018). One of the major reasons for the sample inefficiency of ZOO is its ignorance of the MDP temporal structures. Many recent researches have tried to combine ZOO and first-order

¹School of Vehicle and Mobility, Tsinghua University, Beijing, China ²Institute for Interdisciplinary Information Sciences, Tsinghua University, Beijing, China. Correspondence to: Shengbo Eben Li <lishbo@tsinghua.edu.cn>.

MDP-based RL into hybrid methods, e.g., run evolutionary algorithms in parallel with off-policy RL algorithms and optimize the population of policies with information from both sides (Khadka & Tumer, 2018; Pourchot & Sigaud, 2018; Bodnar et al., 2020), or inject parameter noise into existing RL algorithms for efficient exploration (Plappert et al., 2018; Fortunato et al., 2018). However, existing hybrid methods still conduct first-order gradient-based policy improvement (at least as a part), which reimposes differentiable requirement on the policy.

In this paper, we propose the Zeroth-Order Actor-Critic algorithm (ZOAC), which unifies first-order and zeroth-order RL methods into an actor-critic architecture by conducting first-order PEV to update the critic and zeroth-order PIM to update the actor. In such a way, complementary advantages of both methods are preserved, e.g., wide adaptability to policy parameterization, robustness seeking property, state-dependent and temporally-extended exploration. We modify the rollouts collection strategy from episode-wise perturbation as in traditional zeroth-order methods to timestep-wise perturbation for better exploration, and derive the zeroth-order policy gradient under this setting. We point out that a critic network can be introduced to estimate the state-value function and trade-off between bias and variance. We then propose a practical algorithm that utilizes several parallelized rollout workers and alternates between first-order PEV and zeroth-order PIM based on generated experiences in each iteration. We evaluate ZOAC on a range of challenging continuous control benchmarks from OpenAI gym (Brockman et al., 2016), using different types of policies, including linear policies and neural networks with full or compact architectures. Experiment results show that ZOAC outperforms zeroth-order and first-order baseline algorithms in sample efficiency, final performance, and the robustness of the learned policies. Furthermore, we conduct ablation studies to demonstrate the indispensable contribution of the modified rollouts collection strategy and the introduced critic network to ZOAC.

2. Related Work

ZOO and its applications in RL. At each iteration, ZOO samples several random directions from a certain distribution, and then the distribution is updated according to the evaluation results over these directions. Sehnke et al. (2010) derive parameter-exploring policy gradients (PGPE) for episodic RL problems, which has reduced variance and higher performance than vanilla policy gradient. Salimans et al. (2017) and Such et al. (2017) propose highly scalable evolution strategies (ES) and genetic algorithms (GA) respectively, both of which can be applied to deep neural networks and achieve competitive performance with MDP-based RL algorithms. Mania et al. (2018) propose

augmented random search (ARS), which applied ZOO to linear policies with techniques including observation normalization, reward scaling, top performing directions sifting, and achieve astonishing performance on RL benchmarks considering its simplicity. ZOO has regained popularity in recent years because of its special advantages when applied in RL, including wide adaptability to policy parameterization (e.g., deterministic or stochastic, differentiable or non-differentiable), robustness seeking property, state-dependent and temporally-extended exploration.

Improved techniques for ZOO. The main limitation of ZOO is its high sample complexity. Researchers have proposed various improved techniques for ZOO from different perspectives. One way is to adopt advanced Monte Carlo sampling methods to reduce variance of the zeroth-order gradient estimation, e.g., antithetic sampling (Sehnke et al., 2010; Salimans et al., 2017; Mania et al., 2018), orthogonal and Quasi Monte Carlo exploration (Choromanski et al., 2018). Constructing control variates (i.e., subtracting a baseline) is another popular variance reduction technique. Sehnke et al. (2010) adopt a moving-average baseline in PGPE heuristically, while Zhao et al. (2011) derive the optimal baseline for PGPE in an analytical form that minimizes the variance. Moreover, the sample complexity of zeroth-order methods will further increase with the dimension of the optimization problem (Nesterov & Spokoiny, 2017), therefore some researches aim to identify a low-dimensional search space and guide the search towards faster convergence. Guided ES (Maheswaranathan et al., 2019) and ASEBO (Choromanski et al., 2019) are proposed based on a similar idea: to identify linear subspaces and adapt the search distribution from recent history of descent directions. Sener & Koltun (2020) propose LMRS, which jointly learns the underlying subspace represented by neural networks and optimizes the objective function.

Hybridization of ZOO and first-order MDP-based RL.

These two methods have complementary advantages when applied to RL problems, and recent researches have tried to combine them for better performance. Khadka & Tumer (2018) propose the ERL framework that runs evolutionary algorithms (EA) and DDPG (Lillicrap et al., 2015) concurrently with bidirectional information flow, i.e., the DDPG agent is trained with experiences generated by the EA population and reinserted into the population periodically to guide the evolution process. CEM-RL (Pourchot & Sigaud, 2018) and Proximal Distilled ERL (Bodnar et al., 2020) adopt similar hybridization framework, but use different algorithms as components and improve training techniques. Fortunato et al. (2018) and Plappert et al. (2018) inject parameter noises into existing first-order MDP-based RL algorithms to drive more efficient exploration, and demonstrate that existing RL algorithms can indeed benefit from

parameter space exploration through comparative experiments. Some other hybrid methods (Grathwohl et al., 2018; Tang et al., 2020) leverage policy gradient and reparameterization trick to construct control variates, which leads to unbiased, low variance gradient estimators. Our proposed method, however, unifies first-order and zeroth-order methods into an on-policy actor-critic architecture by conducting first-order PEV and zeroth-order PIM alternately in each iteration. The state-value function network does not only serve as a baseline to reduce variance, but also as a critic used for bootstrapping, which leads to reduced variance and accelerated learning (Sutton & Barto, 2018). The policy is updated in a zeroth-order way, which implies wide adaptability to different forms of policies.

3. Preliminaries

3.1. From Policy Gradient to Actor-Critic

In standard MDP-based RL settings, the environment is usually formulated as an MDP defined as $(\mathcal{S}, \mathcal{A}, \mathcal{P}, r)$, where \mathcal{S} is the state space, \mathcal{A} is the action space, $\mathcal{P} : \mathcal{S} \times \mathcal{A} \times \mathcal{S} \rightarrow \mathbb{R}$ is the transition probability matrix, $r : \mathcal{S} \times \mathcal{A} \rightarrow \mathbb{R}$ is the reward function. The return is defined as the total discounted future reward $G_t = \sum_{i=0}^{\infty} \gamma^i r(s_{t+i}, a_{t+i})$, where $\gamma \in (0, 1)$ is the discounting factor. The behavior of the agent is controlled by a policy $\pi(a|s) : \mathcal{S} \times \mathcal{A} \rightarrow [0, 1]$, which maps states to a probability distribution over actions. Value function is defined as the expected return under policy π : $V^\pi(s) = \mathbb{E}_{a \sim \pi}[G_t | s_t = s]$ and $Q^\pi(s, a) = \mathbb{E}_{a \sim \pi}[G_t | s_t = s, a_t = a]$. The goal of MDP-based RL is to find an optimal policy that maximizes the expectation of state-value function under a certain state distribution. Denoting a policy parameterized with θ as π_θ , the objective function can be written as:

$$J_{\text{PG}}(\theta) = \mathbb{E}_{s \sim d_0}[V^{\pi_\theta}(s)] \quad (1)$$

where d_0 is the initial state distribution. The policy gradient theorem (Sutton & Barto, 2018) holds for any differentiable policy π_θ . The vanilla policy gradient REINFORCE given by Williams (1992) is as follows:

$$\nabla_\theta J_{\text{PG}}(\theta) = \mathbb{E}_{s_t \sim d_{\pi_\theta}, a_t \sim \pi_\theta}[G_t \nabla_\theta \log \pi_\theta(a_t | s_t)] \quad (2)$$

The discounted state distribution is denoted as $d_{\pi_\theta}(s') := \int_{\mathcal{S}} \sum_{t=0}^{\infty} \gamma^t d_0(s) p(s \rightarrow s', t, \pi_\theta) ds$. Vanilla policy gradient suffers from high variance since it directly uses Monte Carlo return from sampled trajectories. Actor-critic methods improved upon it, which usually introduce a critic network to estimate the value function and serve as a baseline to substitute the expected return G_t with a proper form of advantage function A_t , for example, TD residual (Mnih et al., 2016), or generalized advantage estimation (GAE) (Schulman et al., 2015). However, the above policy gradient based methods can only be applied to differentiable policies, and

may be unavailable when a non-differentiable controller needs to be optimized.

3.2. Evolution Strategies

Existing ZOO methods focus on episodic RL problems with finite horizon and treat them as black-box optimization. In these cases, the length of trajectories is limited and the discounting factor γ is usually set as 1. Evolution strategies (ES) is one of the most popular algorithms of ZOO, which optimizes a Gaussian smoothed objective function:

$$J_{\text{ES}}(\theta) = \mathbb{E}_{\epsilon \sim \mathcal{N}(0, I)} \mathbb{E}_{s \sim d_0}[V^{\pi_\theta + \sigma \epsilon}(s)] \quad (3)$$

where d_0 is the initial state distribution and σ is the standard deviation of the Gaussian noise added to the policy. The ES gradient can be derived using the log-likelihood ratio trick and the probability density function of Gaussian distribution (Nesterov & Spokoiny, 2017):

$$\nabla_\theta J_{\text{ES}}(\theta) = \frac{1}{\sigma} \mathbb{E}_{\epsilon \sim \mathcal{N}(0, I)} \mathbb{E}_{s \sim d_0}[V^{\pi_\theta + \sigma \epsilon}(s) \epsilon] \quad (4)$$

In practice, the expectation over Gaussian distribution can be approximated by sampling n noise samples $\{\epsilon_i\}_{i=1, \dots, n}$, and the corresponding state value $V^{\pi_\theta + \sigma \epsilon_i}$ can be approximated by the episodic return $G_i = \sum_{t=0}^T \gamma^t r(s_t, a_t)$ of the sample trajectory of length T collected with policy $\pi_{\theta + \sigma \epsilon_i}$:

$$\nabla_\theta J_{\text{ES}}(\theta) \approx \frac{1}{n\sigma} \sum_{i=1}^n G_i \epsilon_i \quad (5)$$

The gradient estimator in Equation (5) only relies on the episodic returns of each evaluated random directions, so it is applicable to non-differentiable policies. Besides, each perturbed policy remains deterministic in one trajectory, which leads to temporally-extended exploration. Furthermore, the Gaussian smoothed objective also improves robustness of the learned policies in parameter space.

4. Zeroth-Order Actor-Critic

4.1. From ES to ZOAC

In this section, we will derive an improved zeroth-order gradient combining the actor-critic architecture for policy improvement. We start from improving the sample efficiency and stability of ES. Most of the existing ES methods applied to RL optimize a deterministic policy (Salimans et al., 2017; Mania et al., 2018), where the exploration is driven by parameter perturbation. Without loss of generality, we follow them in the following derivations and algorithm design. A deterministic policy parameterized with θ is denoted as $\pi_\theta : \mathcal{S} \rightarrow \mathcal{A}$, which directly maps states to actions.

In ES, the policy is perturbed in parameter space at the beginning of an episode and remains unchanged throughout

the trajectories. If a large number of random directions n is evaluated, the sample complexity will increase significantly. However, since the zeroth-order gradient is estimated as the weighted sum of several random directions, it exhibits excessively high variance when n is small (Berahas et al., 2021), which may greatly harm the performance. Therefore, it is essential to trade-off this contradictory between sample efficiency and variance.

To encourage sufficient exploration and low variance while maintaining high sample efficiency, here we consider perturbing the policy at every timestep, i.e., the Gaussian noise ϵ is sampled identically and independently at every timesteps. We regard it as a stochastic exploration policy $\beta = \pi_{\theta+\sigma\epsilon}$, where σ is the standard deviation and $\epsilon \sim \mathcal{N}(0, I)$ is Gaussian parameter noise. Our objective is to maximize the expected return obtained by the exploration policy β :

$$J_{\text{ZOAC}}(\theta) = \mathbb{E}_{s \sim d_0}[V^\beta(s)] \quad (6)$$

The zeroth-order policy gradient under this setting can be derived as follows. The proof adopts a similar scheme to (Sutton et al., 2000) and (Silver et al., 2014) and is provided in Appendix A.

Theorem 1. *For MDP that satisfies regularity conditions in Appendix A, zeroth-order policy gradient of Equation (6) can be presented as:*

$$\nabla_\theta J_{\text{ZOAC}}(\theta) = \frac{1}{\sigma} \mathbb{E}_{s_t \sim d_\beta} \mathbb{E}_{\epsilon \sim \mathcal{N}(0, I)} [Q^\beta(s_t, \pi_{\theta+\sigma\epsilon}(s_t)) \epsilon] \quad (7)$$

Similar to on-policy policy gradient methods, we can approximate this gradient via on-policy samples and derive different variants of this zeroth-order policy gradient. We first rewrite it into the form of TD residual:

$$\nabla_\theta J_{\text{ZOAC}}(\theta) = \frac{1}{\sigma} \mathbb{E}_{s_t \sim d_\beta} \mathbb{E}_{\epsilon \sim \mathcal{N}(0, I)} \mathbb{E}_{s_{t+1} \sim \mathcal{P}} [(r(s_t, \pi_{\theta+\sigma\epsilon}(s_t)) + \gamma V^\beta(s_{t+1}) - V^\beta(s_t)) \epsilon] \quad (8)$$

Note that in Eq. (8), $V^\beta(s_t)$ can be subtracted as a baseline for variance reduction because: (1) V^β itself is already an expectation over ϵ and is no longer correlated to the noise ϵ ; (2) the zero mean property of the Gaussian noise ϵ .

Compared to ES which uses unbiased but high variance Monte Carlo return to evaluate each perturbed policy, the performance of each random direction here is estimated by one-step TD residual with low variance. In practice, a common approach is to introduce a critic network $V_w(s)$ to estimate the state-value function V^β , which may lead to high bias in this form of advantage estimation.

To trade-off between bias and variance, we consider extending our derivation further to the case where the behavior policy β runs forward N timesteps with each sampled random noise instead of one timestep only, as shown in Figure 2. Eq. (8) can be extended to the N -step TD residual variant:

$$\nabla_\theta J_{\text{ZOAC}}(\theta) = \frac{1}{\sigma} \mathbb{E}_{s_t \sim d_\beta} \mathbb{E}_{\epsilon \sim \mathcal{N}(0, I)} \mathbb{E}_{\mathcal{P}} \left[\left(\sum_{i=0}^{N-1} \gamma^i r_i + \gamma^N V^\beta(s_{t+N}) - V^\beta(s_t) \right) \epsilon \right] \quad (9)$$

where r_i refers to $r(s_{t+i}, \pi_{\theta+\sigma\epsilon}(s_{t+i}))$ and $\mathbb{E}_{\mathcal{P}}$ means expectation over N -step transition dynamics. Similar to one-step case, the cumulative reward within N step can be estimated from sampled experiences when s_t is the first state of the trajectory fragment collected with a certain perturbed policy $\pi_{\theta+\sigma\epsilon}$. By introducing a critic network and choosing an appropriate length N , this N -step residual advantage function contributes to achieving a good trade-off between the bias and variance.

4.2. Analysis on variance of gradient estimators

We analyze the variance of these two types of gradient estimators, ZOAC gradient and ES gradient. The budget of timestep of one trajectory $N \times H$ is identical for both algorithms: in ZOAC, each perturbed policy run forward N steps, and H is the number of sampled random directions in one trajectory; in ES, only one perturbed policy is sampled and run forward $N \times H$ steps. If we denote the accumulative reward obtained within $N \times H$ timesteps in ES as $\hat{V}_{NH}^{\pi_{\theta+\sigma\epsilon}}$ and the N -step TD residual in ZOAC as $\hat{A}_N^{\pi_{\theta+\sigma\epsilon}}$. We can then estimate the zeroth-order policy gradient according to Equation (4) and (9) respectively:

$$\nabla_\theta \hat{J}_{\text{ES}}(\theta) = \frac{1}{n\sigma} \sum_{i=1}^n \hat{V}_{NH}^{\pi_{\theta+\sigma\epsilon_i}} \epsilon_i \quad (10)$$

$$\nabla_\theta \hat{J}_{\text{ZOAC}}(\theta) = \frac{1}{nH\sigma} \sum_{i=1}^{nH} \hat{A}_N^{\pi_{\theta+\sigma\epsilon_i}} \epsilon_i \quad (11)$$

We now give the upper bound of variance for these two gradient estimators. Following (Zhao et al., 2011), variance is defined as the trace of the covariance matrix of gradient vectors $\text{Var}(\mathbf{g}) = \sum_{l=1}^d \mathbb{E}[g_l^2] - (\mathbb{E}g_l)^2$, where $\mathbf{g} = (g_1, g_2, \dots, g_d)^\top$. We can derive the variance bound as follows if both the reward and the critic network output is bounded. The proof is provided in Appendix B, where vectors are bolded for clarity.

Theorem 2. *If the reward $|r(s, a)| < \alpha$, the critic network output $|V_w(s)| < \beta$, and n trajectories with length of $N \times H$ timesteps are collected in one iteration, the upper bounds of the variance for gradient estimators (Equation (10) and*

(11)) are:

$$\text{Var}[\nabla_\theta \hat{J}_{\text{ES}}(\theta)] \leq \frac{(1 - \gamma^{NH})^2 \alpha^2 d}{n \sigma^2 (1 - \gamma)^2} \quad (12)$$

$$\text{Var}[\nabla_\theta \hat{J}_{\text{ZOAC}}(\theta)] \leq \frac{((1 - \gamma^N)\alpha + (1 - \gamma)(1 + \gamma^N)\beta)^2}{n H \sigma^2 (1 - \gamma)^2} \quad (13)$$

We can compare their variance in a more intuitive way: if $N \times H = 1000$, $\gamma = 0.99$, and assume that $\beta \approx \frac{\alpha}{1-\gamma}$, the difference of variance bounds becomes $\text{Var}[\nabla_\theta \hat{J}_{\text{ZOAC}}(\theta)] - \text{Var}[\nabla_\theta \hat{J}_{\text{ES}}(\theta)] \approx (\frac{4}{H} - 1) \frac{10000 \alpha^2 d}{n \sigma^2}$, which decreases with H and drops below zero when $4 < H \leq 1000$ (i.e., N is smaller than 250). This suggests that although same amount of data is collected, an appropriate rollout length N can indeed reduce variance of the gradient estimators. Besides, both variance bound are inversely proportional to n , which urges us to collect more trajectories.

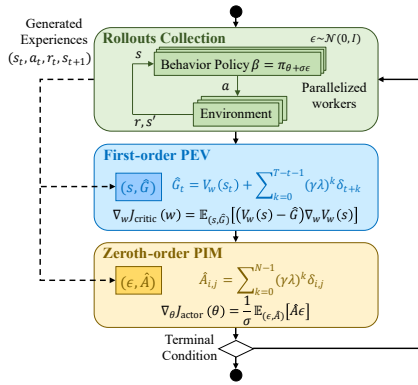


Figure 1. Overall framework of ZOAC

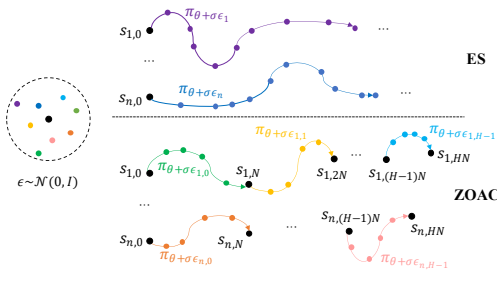


Figure 2. Comparison of rollouts collection strategies (with n parallelized samplers): On the top is ES, which performs episode-wise perturbation; on the bottom is ZOAC, which performs N timestep-wise perturbation.

4.3. Practical Algorithm

We propose the Zeroth-Order Actor-Critic (ZOAC) algorithm, which unifies first-order and zeroth-order methods

into an on-policy actor-critic architecture by conducting rollouts collection with timestep-wise perturbation in parameter space, first-order policy evaluation (PEV) and zeroth-order policy improvement (PIM) alternately in each iteration. The overall framework of ZOAC is shown in Figure 1 and the pseudocode is summarized in Algorithm 1. In each iteration, parallelized workers will collect rollouts in the environment with perturbed policies, then the agent train the critic network to estimate state-value function under the exploration policy, and finally improve the policy along the zeroth-order gradient direction.

Rollouts collection. The rollouts collection strategy is illustrated briefly in Figure 2, which is a parallelized version with n workers. If we denote the t -th state sampled by the i -th worker as $s_{i,t}$, the rollout strategy can be described as: when reaching states in $\{s_{i,jN}\}$, where $j \in \mathbb{N}$, a new random direction $\epsilon_{i,j}$ is sampled and the behavior policy is perturbed; when reaching other states, the deterministic behavior policy remains unchanged. It's worth noting that the notation is only for continuing case where an episode is never done. In episodic tasks, the rollout length $1 \leq N_{i,j} \leq N$ actually varies between different perturbed policies $\pi_{\theta + \sigma \epsilon_{i,j}}$ since an episode may terminate at any time. However, we still use N to denote the rollout length of each perturbed policy for brevity.

A limit case of our proposed strategy is that when N is chosen as the episode length and the critic network is turned off (i.e., $V_w(s) \equiv 0$), the algorithm actually degenerate into ES, since all perturbed policies are evaluated by running a whole episode, and the episodic return is used as the fitness score.

First-order PEV. The state-value function of the behavior policy $V^\beta(s)$ can be estimated by a jointly optimized critic network $V_w(s)$, which aims to minimize the MSE loss between the network output and state-value target. In each iteration, in total $n \times N \times H$ states and the corresponding target values (s, \hat{G}) are calculated and used for critic training. In a trajectory with length T , the target value \hat{G}_t for each state s_t is calculated as (Andrychowicz et al., 2021):

$$\hat{G}_t = V_w(s_t) + \sum_{k=0}^{T-t-1} (\gamma \lambda)^k [r_{t+k} + \gamma V_w(s_{t+k+1}) - V_w(s_{t+k})] \quad (14)$$

where $0 < \lambda < 1$ is a hyperparameter to control the trade-off between bias and variance of the value target. In Figure 1, the one-step TD residual of each state is denoted as δ for simplicity. The objective function of PEV can be written as:

$$J_{\text{critic}}(w) = \mathbb{E}_{(s, \hat{G})} \left[\frac{1}{2} (V_w(s) - \hat{G})^2 \right] \quad (15)$$

In practice, the critic network is constructed as a neural network and updated through several epoches of stochastic

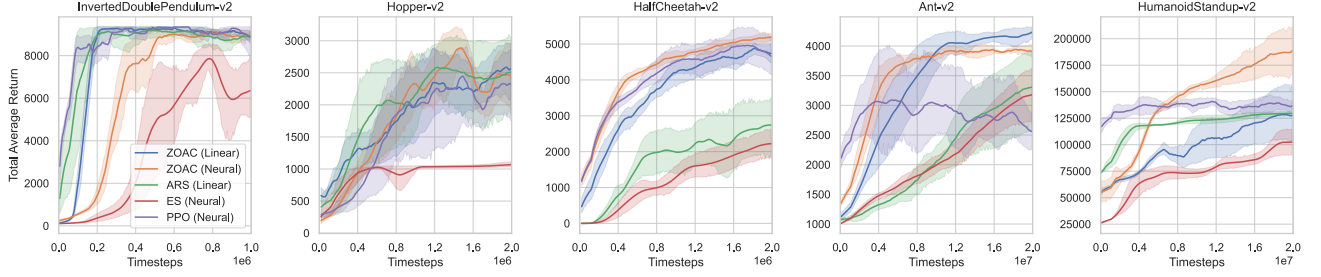


Figure 3. Learning curves on MuJoCo benchmarks. Exploration noise are turned off for evaluation. The solid lines correspond to the mean and the shaded regions to the 95% confidence interval over 5 trials using a fixed set of random seeds. All curves are smoothed uniformly for visual clarity.

gradient descent in each iteration.

Zeroth-order PIM. We calculate the zeroth-order gradient with $n \times H$ random directions and the corresponding advantage function as (ϵ, \hat{A}) . Similar to state value estimation, we leverage the generalized advantage estimation (GAE) trick (Schulman et al., 2015) to further control the bias-variance trade-off. We also perform advantage normalization to ensure consistent gradient length during training. Following the notations in Figure 2, the advantage function can be written as:

$$\hat{A}_N^{\pi_{\theta} + \sigma \epsilon_{i,j}} = \sum_{k=0}^{N-1} (\gamma \lambda)^k [r_{i,jN+k} + \gamma V_w(s_{i,jN+k+1}) - V_w(s_{i,jN+k})] \quad (16)$$

where λ is the same as in Equation (14). The zeroth-order gradient can be then estimated as the weighted sum of the sampled random directions:

$$\nabla_{\theta} J_{\text{actor}}(\theta) \approx \frac{1}{nH\sigma} \sum_{i=1}^n \sum_{j=0}^{H-1} \hat{A}_N^{\pi_{\theta} + \sigma \epsilon_{i,j}} \epsilon_{i,j} \quad (17)$$

5. Experiments

5.1. Performance Evaluation

We evaluate the performance of ZOAC on the MuJoCo continuous control benchmarks (Todorov et al., 2012) in OpenAI Gym (Brockman et al., 2016). We choose Evolution Strategies (ES) (Salimans et al., 2017; Liang et al., 2018) and Augmented Random Search (ARS) (Mania et al., 2018) as zeroth-order baselines and proximal policy optimization (PPO) (Schulman et al., 2017; Raffin et al., 2019) as a first-order on-policy actor-critic baseline.

We use two different types of policies: linear policies for ARS and ZOAC (linear), neural networks with (64, 64) hidden nodes and tanh nonlinearities for ES, PPO and ZOAC (neural). For a fair comparison, we enable observation

normalization for all methods, which has been proved effective no matter in first-order methods or zeroth-order methods (Mania et al., 2018; Andrychowicz et al., 2021). When using neural networks as actors, we also use layer normalization (Ba et al., 2016) in ZOAC and virtual batch normalization in ES (Salimans et al., 2017). Both of them ensure the diversity of behaviors among the population, while the former is less computationally expensive. We summarize the implementation details of ZOAC in Appendix D and follow the recommended hyperparameter settings listed in the related papers or code repositories.

Figure 3 presents the learning curves on four continuous control tasks. Additional results are attached in E, including Table 3 summarizing max total average return within the timestep threshold over 5 trials, and Figure 8 showing state-value estimation difference $V_w(s) - V^{\pi_{\theta}}(s)$ during training.

ZOAC matches or outperforms baseline algorithms across tasks in learning speed, final performance, and variance over trials. One thing worth mentioning is that both the zeroth-order baseline methods perform reward shaping to resolve the local optima problem: ARS subtracts the survival bonus from rewards (1 in Hopper and Ant), while ES transforms the episodic returns into rankings. Although these tricks improve the performance, they also alter the update directions of the policies and make it difficult to determine what is the real objective function being optimized. ZOAC, however, surpasses ES and ARS without relying on specific exploration tricks, which can be attributed to the introduction of critic network and the construction of advantage estimations in policy improvement.

Robustness Comparison. The objective function of ZOAC aims to maximize the expected state-value of the stochastic behavior policy that contains parameter noise all the time, which intuitively encourages the agent to find a wider optima and leads to better generalization and robustness. Hence, we evaluate the learned policies after convergence under two types of noise, observation noise and parameter noise. Extra observation noise is added to the

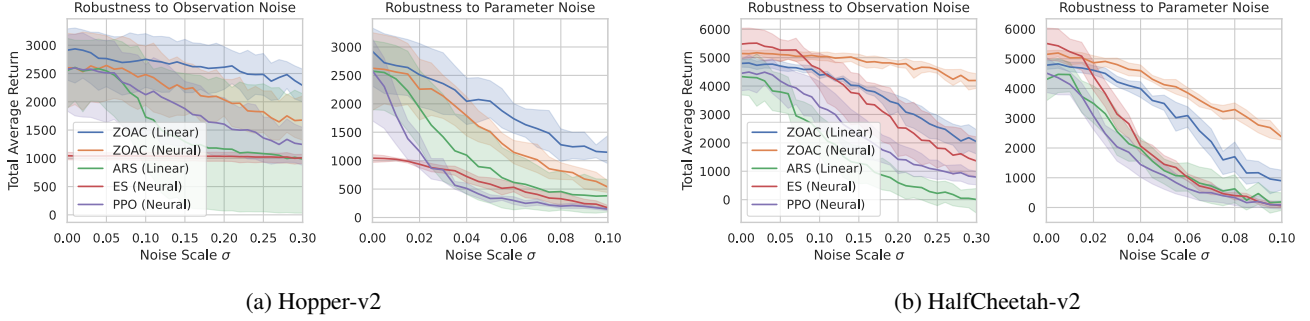


Figure 4. Robustness comparison of the learned policies on observation noise and parameter noise.

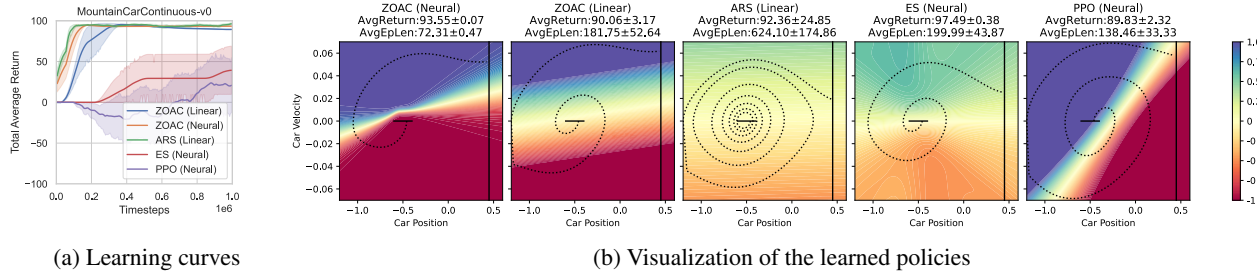


Figure 5. Results on MountainCarContinuous-v0: (a) Learning curves; (b) Visualization of the learned policies. Color represents the action output, from -1.0 (red) to 1.0 (blue). The horizontal lines in solid indicate the initial car position distribution $x \sim U(-0.6, -0.4)$, and the vertical lines in solid indicate the goal $x > 0.45$. The dashed curves are trajectories starting from the same initial state.

normalized observation at each timestep, which leads to a slightly different objective function surface. Extra parameter noise is added at the beginning of each trajectories, which pushes the learned policy to its neighborhood. The result in HalfCheetah-v2 and Hopper-v2 is presented in Figure 4. Results show that in general the policies learned by ZOAC, no matter linear ones or neural ones, possess higher robustness and suffer much milder performance degradation rate under both observation noise and parameter noise, which can be ascribed to the robustness-seeking property of our method.

Visualization of the learned policies. In order to intuitively observe the behaviors of the learned policies, we apply all methods on MountainCarContinuous-v0, in which the car is rewarded $+100$ only when it achieves the goal and penalized by the action output at every timestep. Policy gradient methods usually struggle on this problem because the reward is sparse and delayed, while zeroth-order methods can better handle reward sparsity by nature. We plot the learning curves over 10 trials in Figure 5a and it can be seen that ZOAC can learn a good solution consistently while PPO and ES get stuck occasionally. We also visualize the learned policies in Figure 5a. Among the learned policies, the neural policy learned by ES obtains the highest average return, while the neural policy learned by ZOAC obtains the second highest average return within the shortest episode length. The latter has a similar but much steeper terrain

compared to the former one and implies a larger control action in most areas. As for linear policies, the one learned by ZOAC also tends to achieve the goal in a shorter episode length than the one learned by ARS. We attribute this to the usage of discounting factor, which pushes the agent to perform higher actions and achieve the goal as early as possible. ZOAC outperforms PPO both in final performance and training stability over different random seeds, due to its state-dependent exploration, which is more efficient than action noise and is essential to solve this task.

Learning compact policies. The derivative-free nature of ZOAC allows us to estimate the zeroth-order policy gradient to improve the policy without considering the specific policy architecture. Hence, ZOAC can be applied seamlessly to arbitrary parameterized policies in theory, no matter differentiable or not. We further apply ZOAC on two more neural policies with compact structures: Toeplitz networks that adopt parameter sharing (Choromanski et al., 2018) and masked networks that automatically masking out redundant parameters (Lenc et al., 2019; Song et al., 2021). The detailed introduction of the compact network architecture is attached in Appendix F. We perform additional experiments on two high-dimensional environments. Results in Figure 6 and Table 1 show that ZOAC successfully trains these compact policies. Although the performance is slightly inferior to the full neural policies, it still indicates the high flexibility and of ZOAC in usage.

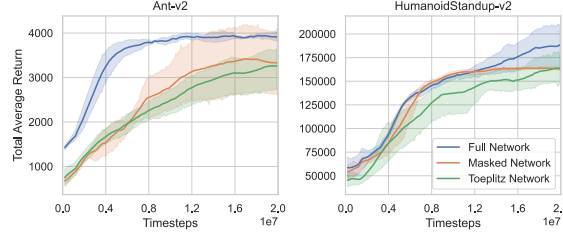


Figure 6. Performance of networks with different architectures

Table 1. Dimension comparison of different networks.

Env.	Ant	Human.Stand.
State space	111	376
Action space	8	17
Full Network	11848	29393
Toeplitz Network	508	791
Maksed Network	1262 ± 69	1342 ± 209

5.2. Ablation Studies

Appropriate rollout length. As illustrated in Section 4.2, choosing appropriate rollout length N of each perturbed policies may achieve a good trade-off between bias and variance. We perform an ablation study to understand the effect of timestep-wise perturbation strategy and choice of N . We compare ZOAC and ARS on HalfCheetah-v2, the former conducting timestep-wise perturbation and the latter conducting episode-wise perturbation. We use linear policies in both methods and set hyperparameters to the same, including the standard deviation of parameter noise σ , the learning rate of policy α_{actor} , and also the budget of timesteps within one iteration. Figure 7a shows the influence of N on performance. Results show that under this setting, both 10 and 20 are good choices for N which lead to better performance, while other two choices, 5 and 50, perform similarly to ARS. Note that here we sample as many experiences as ARS per iteration for comparison, while in practice, the number of timesteps collected in each iteration is highly tunable in ZOAC. In fact, we found that rollout length N in a large range, approximately from 5 to 50, perform quite well across tasks.

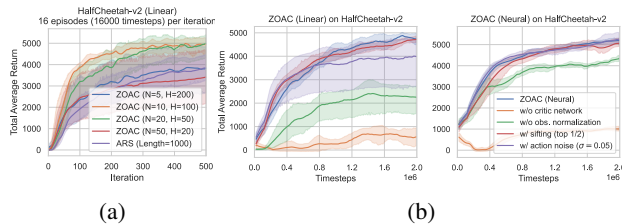


Figure 7. (a) Influence of the rollout length N ; (b) Ablation studies on different components of ZOAC

Analysis on different components. To evaluate the contribution of each individual component and also the potential of additional techniques, we perform ablation studies and present the results in Figure 7b. Results demonstrate that critic network is a crucial part of ZOAC, i.e., N -step accumulative reward without bootstrapping is not sufficient to guide policy improvement. Observation normalization technique is also essential to zeroth-order methods, which helps to generate diverse policies via isotropic Gaussian noise. Mania et al. (2018) propose to use only the top performing directions in policy update to relieve the bad influence of noisy evaluation results and validate its effectiveness on ARS. Here we perform a similar direction sifting technique, using only the directions that have the highest advantage in policy improvement, but it seems not helpful to the learning performance of ZOAC. Besides, additional action noise does not help either, indicating that the exploration driven by parameter noise is sufficient.

6. Conclusion

In this paper, we propose Zeroth-Order Actor-Critic algorithm (ZOAC) that unifies evolution based zeroth-order and policy gradient based first-order methods into an on-policy actor-critic architecture to preserve the advantages from both, including the ability to handle different forms of policies, state-dependent exploration, robustness-seeking property from the former and high sample efficiency from the latter. ZOAC conducts rollouts collection with timestep-wise perturbation in parameter space, first-order policy evaluation (PEV) and zeroth-order policy improvement (PIM) alternately in each iteration. Experimental results in a range of challenging continuous control tasks show the superior performance of ZOAC. Robustness analysis and ablation studies on hyperparameters and components are also performed to show the properties of ZOAC.

Although ZOAC has made great progress compared with state-of-the-art zeroth-order methods and on-policy first-order methods, present version of ZOAC is still based on on-policy architecture and does not reuse samples from previous iteration. The on-policy characteristic gives itself higher stability and convergence and less hyperparameter sensitivity, but also limits the possibility of even higher sample efficiency. We leave the off-policy version of ZOAC and the comparison with off-policy methods like TD3 and SAC as our near future work. Moreover, our method achieves such improvement while still using traditional isotropic Gaussian noise for perturbation, so in principle those improved sampling techniques from ZOO community can be further integrated, e.g., Monte Carlo sampling techniques, low-dimensional subspace identification, adaptive perturbation scale, which may lead to even higher performance.

References

Andrychowicz, M., Raichuk, A., Stańczyk, P., Orsini, M., Girgin, S., Marinier, R., Hussenot, L., Geist, M., Pietquin, O., Michalski, M., Gelly, S., and Bachem, O. What matters for on-policy deep actor-critic methods? a large-scale study. In *International Conference on Learning Representations*, 2021.

Ba, J. L., Kiros, J. R., and Hinton, G. E. Layer normalization. *arXiv preprint arXiv:1607.06450*, 2016.

Berahas, A. S., Cao, L., Choromanski, K., and Scheinberg, K. A theoretical and empirical comparison of gradient approximations in derivative-free optimization. *Foundations of Computational Mathematics*, pp. 1–54, 2021.

Bodnar, C., Day, B., and Lió, P. Proximal distilled evolutionary reinforcement learning. In *Proceedings of the AAAI Conference on Artificial Intelligence*, volume 34, pp. 3283–3290, 2020.

Brockman, G., Cheung, V., Pettersson, L., Schneider, J., Schulman, J., Tang, J., and Zaremba, W. Openai gym. *arXiv preprint arXiv:1606.01540*, 2016.

Choromanski, K., Rowland, M., Sindhwani, V., Turner, R., and Weller, A. Structured evolution with compact architectures for scalable policy optimization. In *International Conference on Machine Learning*, pp. 970–978. PMLR, 2018.

Choromanski, K., Pacchiano, A., Parker-Holder, J., Tang, Y., and Sindhwani, V. From complexity to simplicity: Adaptive es-active subspaces for blackbox optimization. *Advances in Neural Information Processing Systems*, 32: 10299–10309, 2019.

Conti, E., Madhavan, V., Such, F. P., Lehman, J., Stanley, K. O., and Clune, J. Improving exploration in evolution strategies for deep reinforcement learning via a population of novelty-seeking agents. In *Proceedings of the 32nd International Conference on Neural Information Processing Systems*, pp. 5032–5043, 2018.

Fortunato, M., Azar, M. G., Piot, B., Menick, J., Hessel, M., Osband, I., Graves, A., Mnih, V., Munos, R., Hassabis, D., Pietquin, O., Blundell, C., and Legg, S. Noisy networks for exploration. In *International Conference on Learning Representations*, 2018.

Grathwohl, W., Choi, D., Wu, Y., Roeder, G., and Duvenaud, D. Backpropagation through the void: Optimizing control variates for black-box gradient estimation. In *International Conference on Learning Representations*, 2018.

Ha, D. and Schmidhuber, J. World models. *arXiv preprint arXiv:1803.10122*, 2018.

Kendall, A., Hawke, J., Janz, D., Mazur, P., Reda, D., Allen, J.-M., Lam, V.-D., Bewley, A., and Shah, A. Learning to drive in a day. In *2019 International Conference on Robotics and Automation (ICRA)*, pp. 8248–8254. IEEE, 2019.

Khadka, S. and Tumer, K. Evolution-guided policy gradient in reinforcement learning. In *Proceedings of the 32nd International Conference on Neural Information Processing Systems*, pp. 1196–1208, 2018.

Lehman, J., Chen, J., Clune, J., and Stanley, K. O. Es is more than just a traditional finite-difference approximator. In *Proceedings of the Genetic and Evolutionary Computation Conference*, pp. 450–457, 2018.

Lenc, K., Elsen, E., Schaul, T., and Simonyan, K. Non-differentiable supervised learning with evolution strategies and hybrid methods. *arXiv preprint arXiv:1906.03139*, 2019.

Liang, E., Liaw, R., Nishihara, R., Moritz, P., Fox, R., Goldberg, K., Gonzalez, J., Jordan, M., and Stoica, I. Rllib: Abstractions for distributed reinforcement learning. In *International Conference on Machine Learning*, pp. 3053–3062. PMLR, 2018.

Lillicrap, T. P., Hunt, J. J., Pritzel, A., Heess, N., Erez, T., Tassa, Y., Silver, D., and Wierstra, D. Continuous control with deep reinforcement learning. *arXiv preprint arXiv:1509.02971*, 2015.

Maheswaranathan, N., Metz, L., Tucker, G., Choi, D., and Sohl-Dickstein, J. Guided evolutionary strategies: Augmenting random search with surrogate gradients. In *International Conference on Machine Learning*, pp. 4264–4273. PMLR, 2019.

Mania, H., Guy, A., and Recht, B. Simple random search of static linear policies is competitive for reinforcement learning. In *Proceedings of the 32nd International Conference on Neural Information Processing Systems*, pp. 1805–1814, 2018.

Mnih, V., Kavukcuoglu, K., Silver, D., Rusu, A. A., Veness, J., Bellemare, M. G., Graves, A., Riedmiller, M., Fidjeland, A. K., Ostrovski, G., et al. Human-level control through deep reinforcement learning. *nature*, 518(7540): 529–533, 2015.

Mnih, V., Badia, A. P., Mirza, M., Graves, A., Lillicrap, T., Harley, T., Silver, D., and Kavukcuoglu, K. Asynchronous methods for deep reinforcement learning. In *International conference on machine learning*, pp. 1928–1937. PMLR, 2016.

Moritz, P., Nishihara, R., Wang, S., Tumanov, A., Liaw, R., Liang, E., Elibol, M., Yang, Z., Paul, W., Jordan, M. I., et al. Ray: A distributed framework for emerging {AI} applications. In *13th {USENIX} Symposium on Operating Systems Design and Implementation ({OSDI} 18)*, pp. 561–577, 2018.

Nesterov, Y. and Spokoiny, V. Random gradient-free minimization of convex functions. *Foundations of Computational Mathematics*, 17(2):527–566, 2017.

Plappert, M., Houthooft, R., Dhariwal, P., Sidor, S., Chen, R. Y., Chen, X., Asfour, T., Abbeel, P., and Andrychowicz, M. Parameter space noise for exploration. In *International Conference on Learning Representations*, 2018.

Pourchot, A. and Sigaud, O. Cem-rl: Combining evolutionary and gradient-based methods for policy search. *arXiv preprint arXiv:1810.01222*, 2018.

Pourchot, A., Perrin, N., and Sigaud, O. Importance mixing: Improving sample reuse in evolutionary policy search methods. *arXiv preprint arXiv:1808.05832*, 2018.

Qian, H. and Yu, Y. Derivative-free reinforcement learning: A review. *arXiv preprint arXiv:2102.05710*, 2021.

Raffin, A., Hill, A., Ernestus, M., Gleave, A., Kanervisto, A., and Dormann, N. Stable baselines3. *GitHub repository*, 2019.

Risi, S. and Stanley, K. O. Deep neuroevolution of recurrent and discrete world models. In *Proceedings of the Genetic and Evolutionary Computation Conference*, pp. 456–462, 2019.

Salimans, T., Ho, J., Chen, X., Sidor, S., and Sutskever, I. Evolution strategies as a scalable alternative to reinforcement learning. *arXiv preprint arXiv:1703.03864*, 2017.

Schulman, J., Moritz, P., Levine, S., Jordan, M., and Abbeel, P. High-dimensional continuous control using generalized advantage estimation. *arXiv preprint arXiv:1506.02438*, 2015.

Schulman, J., Wolski, F., Dhariwal, P., Radford, A., and Klimov, O. Proximal policy optimization algorithms. *arXiv preprint arXiv:1707.06347*, 2017.

Sehnke, F., Osendorfer, C., Rückstieß, T., Graves, A., Peters, J., and Schmidhuber, J. Parameter-exploring policy gradients. *Neural Networks*, 23(4):551–559, 2010.

Sener, O. and Koltun, V. Learning to guide random search. In *International Conference on Learning Representations*, 2020.

Sigaud, O. and Stulp, F. Policy search in continuous action domains: an overview. *Neural Networks*, 113:28–40, 2019.

Silver, D., Lever, G., Heess, N., Degris, T., Wierstra, D., and Riedmiller, M. Deterministic policy gradient algorithms. In *International conference on machine learning*, pp. 387–395. PMLR, 2014.

Song, X., Choromanski, K., Parker-Holder, J., Tang, Y., Zhang, Q., Peng, D., Jain, D., Gao, W., Pacchiano, A., Sarlos, T., and Yang, Y. Es-enas: Blackbox optimization over hybrid spaces via combinatorial and continuous evolution, 2021.

Stanley, K. O., Clune, J., Lehman, J., and Miikkulainen, R. Designing neural networks through neuroevolution. *Nature Machine Intelligence*, 1(1):24–35, 2019.

Such, F. P., Madhavan, V., Conti, E., Lehman, J., Stanley, K. O., and Clune, J. Deep neuroevolution: Genetic algorithms are a competitive alternative for training deep neural networks for reinforcement learning. *arXiv preprint arXiv:1712.06567*, 2017.

Sutton, R. S. and Barto, A. G. *Reinforcement learning: An introduction*. MIT press, 2018.

Sutton, R. S., McAllester, D. A., Singh, S. P., and Mansour, Y. Policy gradient methods for reinforcement learning with function approximation. In *Advances in neural information processing systems*, pp. 1057–1063, 2000.

Tang, Y., Choromanski, K., and Kucukelbir, A. Variance reduction for evolution strategies via structured control variates. In *International Conference on Artificial Intelligence and Statistics*, pp. 646–656. PMLR, 2020.

Todorov, E., Erez, T., and Tassa, Y. Mujoco: A physics engine for model-based control. In *2012 IEEE/RSJ International Conference on Intelligent Robots and Systems*, pp. 5026–5033. IEEE, 2012.

Williams, R. J. Simple statistical gradient-following algorithms for connectionist reinforcement learning. *Machine learning*, 8(3):229–256, 1992.

Zhao, T., Hachiya, H., Niu, G., and Sugiyama, M. Analysis and improvement of policy gradient estimation. *Advances in Neural Information Processing Systems*, 24:262–270, 2011.

Zeroth-Order Actor-Critic: Supplementary Material

A. Proof of Theorem 1

Regularity conditions 1: $p(s'|s, a), \pi_\theta(s), r(s, a), d_0(s)$ are continuous in all parameters and variables s, a, s' .

Theorem 1. For MDP that satisfies regularity conditions 1, zeroth-order policy gradient of Equation (6) can be presented as:

$$\nabla_\theta J_{ZOAC}(\theta) = \frac{1}{\sigma} \mathbb{E}_{s_t \sim d_\beta} \mathbb{E}_{\epsilon \sim \mathcal{N}(0, I)} [Q^\beta(s_t, \pi_{\theta+\sigma\epsilon}(s_t)) \epsilon]$$

The following proof follows the policy gradient theorem proved by Sutton et al. (2000) and the deterministic policy gradient theorem proved by Silver et al. (2014). The above regularity conditions, together with Leibniz integral rule and Fubini's theorem, enable us to exchange derivatives and integrals, and the order of integration whenever necessary and we do not repeat during the proof.

Proof.

$$\begin{aligned} \nabla_\theta V^\beta(s) &= \nabla_\theta \mathbb{E}_{\epsilon_1 \sim \mathcal{N}(0, I)} [Q^\beta(s, \pi_{\theta+\sigma\epsilon_1}(s))] \\ &= \nabla_\theta \mathbb{E}_{\epsilon_1 \sim \mathcal{N}(0, I)} \left[r(s, \pi_{\theta+\sigma\epsilon_1}(s)) + \int_{\mathcal{S}} \gamma p(s'|s, \pi_{\theta+\sigma\epsilon_1}(s)) V^\beta(s') ds' \right] \\ &= \frac{1}{\sigma} \mathbb{E}_{\epsilon_1 \sim \mathcal{N}(0, I)} \left[\left(r(s, \pi_{\theta+\sigma\epsilon_1}(s)) + \int_{\mathcal{S}} \gamma p(s'|s, \pi_{\theta+\sigma\epsilon_1}(s)) V^\beta(s') ds' \right) \epsilon_1 \right] \\ &\quad + \mathbb{E}_{\epsilon_1 \sim \mathcal{N}(0, I)} \int_{\mathcal{S}} \gamma p(s'|s, \pi_{\theta+\sigma\epsilon_1}(s)) \nabla_\theta V^\beta(s') ds' \\ &= \frac{1}{\sigma} \mathbb{E}_{\epsilon_1 \sim \mathcal{N}(0, I)} [Q^\beta(s, \pi_{\theta+\sigma\epsilon_1}(s)) \epsilon_1] \\ &\quad + \mathbb{E}_{\epsilon_1 \sim \mathcal{N}(0, I)} \int_{\mathcal{S}} \gamma p(s \rightarrow s', 1, \pi_{\theta+\sigma\epsilon_1}) \nabla_\theta V^\beta(s') ds' \end{aligned}$$

Note that in the above derivation, we use the zeroth-order gradient trick as in Equation (4) in some of the terms, i.e.:

$$\nabla_\theta \mathbb{E}_{\epsilon \sim \mathcal{N}(0, I)} f(\theta + \sigma\epsilon) = \frac{1}{\sigma} \mathbb{E}_{\epsilon \sim \mathcal{N}(0, I)} [f(\theta + \sigma\epsilon) \epsilon]$$

We continue to unroll the recursive representation of $\nabla_\theta V^\beta(s)$:

$$\begin{aligned} \nabla_\theta V^\beta(s) &= \frac{1}{\sigma} \mathbb{E}_{\epsilon_1 \sim \mathcal{N}(0, I)} [Q^\beta(s, \pi_{\theta+\sigma\epsilon_1}(s)) \epsilon_1] \\ &\quad + \frac{1}{\sigma} \mathbb{E}_{\epsilon_1 \sim \mathcal{N}(0, I)} \int_{\mathcal{S}} \gamma p(s \rightarrow s', 1, \pi_{\theta+\sigma\epsilon_1}) \mathbb{E}_{\epsilon_2 \sim \mathcal{N}(0, I)} [Q^\beta(s', \pi_{\theta+\sigma\epsilon_2}(s')) \epsilon_2] ds' \\ &\quad + \mathbb{E}_{\epsilon_1 \sim \mathcal{N}(0, I)} \int_{\mathcal{S}} \gamma p(s \rightarrow s', 1, \pi_{\theta+\sigma\epsilon_1}) \mathbb{E}_{\epsilon_2 \sim \mathcal{N}(0, I)} \int_{\mathcal{S}} \gamma p(s' \rightarrow s'', 1, \pi_{\theta+\sigma\epsilon_2}) \nabla_\theta V^\beta(s'') ds'' ds' \end{aligned}$$

Since the behavior policy β is exactly the stochastic version of π_θ with Gaussian parameter noise ϵ sampled i.i.d. at every timesteps, we can rewrite and continue to iterate the above formula:

$$\begin{aligned}
 \nabla_{\theta} V^{\beta}(s) &= \frac{1}{\sigma} \mathbb{E}_{\epsilon \sim \mathcal{N}(0, I)} [Q^{\beta}(s, \pi_{\theta+\sigma\epsilon}(s))\epsilon] \\
 &\quad + \int_{\mathcal{S}} \gamma p(s \rightarrow s', 1, \beta) \frac{1}{\sigma} \mathbb{E}_{\epsilon \sim \mathcal{N}(0, I)} [Q^{\beta}(s', \pi_{\theta+\sigma\epsilon}(s'))\epsilon] ds' \\
 &\quad + \int_{\mathcal{S}} \gamma^2 p(s \rightarrow s', 2, \beta) \nabla_{\theta} V^{\beta}(s') ds' \\
 &= \dots \\
 &= \int_{\mathcal{S}} \sum_{t=0}^{\infty} \gamma^t p(s \rightarrow s', t, \beta) \frac{1}{\sigma} \mathbb{E}_{\epsilon \sim \mathcal{N}(0, I)} [Q^{\beta}(s', \pi_{\theta+\sigma\epsilon}(s'))\epsilon] ds'
 \end{aligned}$$

Now we can derive the zeroth-order policy gradient by taking the expectation over initial state distribution:

$$\begin{aligned}
 \nabla_{\theta} J_{\text{ZOAC}}(\theta) &= \nabla_{\theta} \mathbb{E}_{s \sim d_0} [V^{\beta}(s)] \\
 &= \int_{\mathcal{S}} d_0(s) \nabla_{\theta} V^{\beta}(s) ds \\
 &= \int_{\mathcal{S}} \int_{\mathcal{S}} \sum_{t=0}^{\infty} \gamma^t d_0(s) p(s \rightarrow s', t, \beta) \frac{1}{\sigma} \mathbb{E}_{\epsilon \sim \mathcal{N}(0, I)} [Q^{\beta}(s', \pi_{\theta+\sigma\epsilon}(s'))\epsilon] ds' ds \\
 &= \frac{1}{\sigma} \int_{\mathcal{S}} d_{\beta}(s) \mathbb{E}_{\epsilon \sim \mathcal{N}(0, I)} [Q^{\beta}(s, \pi_{\theta+\sigma\epsilon}(s))\epsilon] ds \\
 &= \frac{1}{\sigma} \mathbb{E}_{s \sim d_{\beta}} \mathbb{E}_{\epsilon \sim \mathcal{N}(0, I)} [Q^{\beta}(s, \pi_{\theta+\sigma\epsilon}(s))\epsilon]
 \end{aligned}$$

□

B. Proof of Theorem 2

Theorem 2. *If the reward $|r(s, a)| < \alpha$, the critic network output $|V_w(s)| < \beta$, and n trajectories with length of $N \times H$ timesteps are collected in one iteration, the upper bounds of the variance of gradient estimators (Equation (10) and (11)) are:*

$$\begin{aligned}
 \text{Var}[\nabla_{\theta} \hat{J}_{\text{ES}}(\theta)] &\leq \frac{(1 - \gamma^{NH})^2 \alpha^2 d}{n \sigma^2 (1 - \gamma)^2} \\
 \text{Var}[\nabla_{\theta} \hat{J}_{\text{ZOAC}}(\theta)] &\leq \frac{((1 - \gamma^N)\alpha + (1 - \gamma)(1 + \gamma^N)\beta)^2 d}{n H \sigma^2 (1 - \gamma)^2}
 \end{aligned}$$

Proof. (1) Variance bound for ES gradient estimators

Under the setting described in Section 4.2, the state-value under policy $\pi_{\theta+\sigma\epsilon}$ is estimated by the accumulative return over NH timesteps, which is denoted as $\hat{V}_{NH}^{\pi_{\theta+\sigma\epsilon}}$. The isotropic Gaussian noise added to the policy can be presented as

$\epsilon = (\epsilon_1, \epsilon_2, \dots, \epsilon_d)^\top$, where $\epsilon_l \sim \mathcal{N}(0, 1)$, $l \in \{1, 2, \dots, d\}$.

$$\begin{aligned}
 \text{Var}[\hat{V}_{NH}^{\pi_{\theta+\sigma\epsilon}} \epsilon] &\leq \sum_{l=1}^d \mathbb{E}[(\hat{V}_{NH}^{\pi_{\theta+\sigma\epsilon}} \epsilon_l)^2] \\
 &= \sum_{l=1}^d \int p(\epsilon_l) \left(\sum_{t=1}^{NH} \gamma^{t-1} r(s_t, a_t) \right)^2 \epsilon_l^2 d\epsilon_l \\
 &\leq \sum_{l=1}^d \int p(\epsilon_l) \left(\sum_{t=1}^{NH} \gamma^{t-1} \alpha \right)^2 \epsilon_l^2 d\epsilon_l \\
 &= \frac{(1 - \gamma^{NH})^2 \alpha^2}{(1 - \gamma)^2} \sum_{l=1}^d \int p(\epsilon_l) \epsilon_l^2 d\epsilon_l \\
 &= \frac{(1 - \gamma^{NH})^2 \alpha^2}{(1 - \gamma)^2} \sum_{l=1}^d \mathbb{E}_{\epsilon_l \sim \mathcal{N}(0, 1)} \epsilon_l^2 \\
 &= \frac{(1 - \gamma^{NH})^2 \alpha^2 d}{(1 - \gamma)^2}
 \end{aligned}$$

The last equality holds because $\epsilon_l^2 \sim \chi^2(1)$ when $\epsilon_l \sim \mathcal{N}(0, 1)$, and $\mathbb{E}[\epsilon_l^2] = 1$ for all l . Since n random directions are sampled and evaluated, the ES gradient estimator is given according to Equation (10):

$$\nabla_{\theta} \hat{J}_{\text{ES}}(\theta) = \frac{1}{n\sigma} \sum_{i=1}^n \hat{V}_{NH}^{\pi_{\theta+\sigma\epsilon_i}} \epsilon_i^2$$

Therefore the variance bound for ES can be derived as in Theorem 1:

$$\begin{aligned}
 \text{Var}[\nabla_{\theta} \hat{J}_{\text{ES}}(\theta)] &= \frac{1}{n\sigma^2} \text{Var}[\hat{V}_{NH}^{\pi_{\theta+\sigma\epsilon}} \epsilon] \\
 &\leq \frac{(1 - \gamma^{NH})^2 \alpha^2 d}{n\sigma^2 (1 - \gamma)^2}
 \end{aligned}$$

(2) Variance bound for ZOAC gradient estimators

Under the setting described in Section 4.2, the performance under policy $\pi_{\theta+\sigma\epsilon}$ is estimated by the N -step TD residual, which is denoted as $\hat{A}_N^{\pi_{\theta+\sigma\epsilon}}$. The isotropic Gaussian noise ϵ is added to the policy as well.

$$\begin{aligned}
 \text{Var}[\hat{A}_N^{\pi_{\theta+\sigma\epsilon}} \epsilon] &\leq \sum_{l=1}^d \mathbb{E}[(\hat{A}_N^{\pi_{\theta+\sigma\epsilon}} \epsilon_l)^2] \\
 &= \sum_{l=1}^d \int p(\epsilon_l) \left(\sum_{t=1}^N \gamma^{t-1} r(s_t, a_t) + \gamma^N V_w(s_{t+N}) - V_w(s_t) \right)^2 \epsilon_l^2 d\epsilon_l \\
 &\leq \sum_{l=1}^d \int p(\epsilon_l) \left(\sum_{t=1}^N \gamma^{t-1} \alpha + (1 + \gamma^N) \beta \right)^2 \epsilon_l^2 d\epsilon_l \\
 &= \left(\frac{(1 - \gamma^N) \alpha + (1 - \gamma)(1 + \gamma^N) \beta}{(1 - \gamma)} \right)^2 \sum_{l=1}^d \int p(\epsilon_l) \epsilon_l^2 d\epsilon_l \\
 &= \left(\frac{(1 - \gamma^N) \alpha + (1 - \gamma)(1 + \gamma^N) \beta}{(1 - \gamma)} \right)^2 d
 \end{aligned}$$

Totally $n \times H$ random directions are sampled and evaluated, and the ZOAC gradient estimator is given according to Equation (11):

$$\nabla_{\theta} \hat{J}_{\text{ZOAC}}(\theta) \approx \frac{1}{nH\sigma} \sum_{i=1}^{nH} \hat{A}_N^{\pi_{\theta} + \sigma \epsilon_i} \epsilon_i$$

Therefore the variance bound for ZOAC can be derived:

$$\begin{aligned} \text{Var}[\nabla_{\theta} \hat{J}_{\text{ZOAC}}(\theta)] &= \frac{1}{nH\sigma^2} \text{Var}[\hat{A}_N^{\pi_{\theta} + \sigma \epsilon} \epsilon] \\ &\leq \frac{((1 - \gamma^N)\alpha + (1 - \gamma)(1 + \gamma^N)\beta)^2 d}{nH\sigma^2(1 - \gamma)^2} \end{aligned}$$

□

C. Pseudocode of ZOAC

Algorithm 1 Zeroth-Order Actor-Critic (ZOAC)

```

1: Initialize: policy parameters  $\theta$ , critic network parameters  $w$ 
2: for each iteration do
3:   for each worker  $i = 1, 2, \dots, n$  do
4:     for  $j = 0, 1, \dots, H - 1$  do
5:       Sample  $\epsilon_{i,j} \sim \mathcal{N}(0, I)$ 
6:       Run perturbed policy  $\pi_{\theta + \sigma \epsilon_{i,j}}$  in environment for  $N$  timesteps
7:       Compute advantage function  $\hat{A}^{\pi_{\theta + \sigma \epsilon_{i,j}}}$  according to Equation (16)
8:     end for
9:     Compute the state-value target  $\hat{G}_t$  for each state  $s_t$  according to Equation (14)
10:   end for
11:   Collect  $(s, \hat{G})$  for critic update and  $(\epsilon, \hat{A})$  for actor update
12:   Update  $w$  with batch size  $L$  through SGD by minimizing Equation (15) for  $M$  epochs
13:   Update  $\theta$  along the zeroth-order gradient direction estimated in Equation (17)
14: end for

```

D. Implementation details

We implemented ZOAC with parallelized workers (Algorithm 1) using the distributed framework Ray (Moritz et al., 2018). We follow the parallelization techniques used in ES (Salimans et al., 2017) and ARS (Mania et al., 2018). Firstly, we created a shared noise table before training starts, then the workers communicate indices in the shared table but not the perturbation vectors, so as to avoid high communication cost. Besides, random seeds for constructing parallelized training environments and the evaluation environment are different and generated from a single seed designated before hand.

We use two different types of policies: linear policies for ARS and ZOAC (linear), neural networks with (64, 64) hidden nodes and tanh nonlinearities for ES, PPO and ZOAC (neural). For actor-critic algorithms, we use neural networks with (256, 256) hidden nodes and tanh nonlinearities as critics to estimate state-value function.

Both the zeroth-order baseline methods perform reward shaping to resolve the local optima problem as described in the original paper: ARS subtracts the survival bonus from rewards (1 in Hopper and Ant), while ES transforms the episodic returns into rankings. ES further discretize the actions to encourage exploration in Hopper but we do not reserve this trick for comparison since discretization will lead to a different policy architecture.

We summarize the hyperparameters used in ZOAC in Table 2 and list their values that are used to produce the results in Figure 3. We tune several important hyperparameters (n, N, H, σ) via coarse grid search and select the best performing setting to produce the final results. During evaluation, exploration noise are turned off and the reported total average return is averaged over 10 episodes.

Table 2. Hyperparameters of ZOAC for the learning curves shown in Figure 3 and 3

Environment	Inv.D.P.-v2		Hopper-v2		HalfCheetah-v2		Ant-v2		Human.Stand.-v2							
Policy type	Linear	Neural	Linear	Neural	Linear	Neural	Linear	Neural	Linear	Neural						
Num. of workers n	4		4	8	4	8			8							
Rollout length N	10		20		20		20		10							
Train frequency H	16		16		16		256		128							
Para. noise std. σ	0.02	0.04	0.04		0.04	0.06			0.03							
Batch size L	64						128									
Num. of epoches M	8						4									
Actor optimizer	Adam($\alpha_{\text{actor}} = 0.005, \beta_1 = 0.9, \beta_2 = 0.999$)					$\alpha_{\text{actor}} = 0.003$										
Critic optimizer	Adam($\alpha_{\text{critic}} = 0.0003, \beta_1 = 0.9, \beta_2 = 0.999$)															
Discount factor γ	0.99															
GAE coeff. λ	0.95															

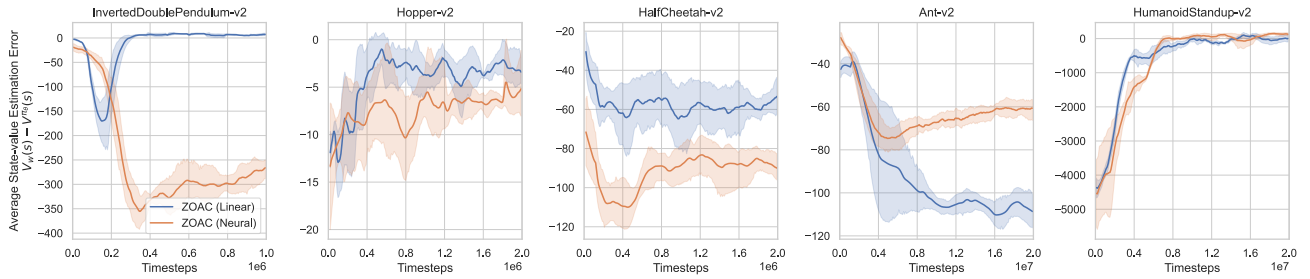


Figure 8. Average state-value estimation difference $V_w(s) - V^{\pi_\theta}(s)$ in evaluation during training in Figure 3. The solid lines correspond to the mean and the shaded regions to the 95% confidence interval over 5 trials using a fixed set of random seeds. All curves are smoothed uniformly for visual clarity.

E. Additional Results

Figure 8 plots the average state-value estimation difference $V_w(s) - V^{\pi_\theta}(s)$ in evaluation during training. Since we turn off the exploration noise for evaluation, which means that the trajectories are collected under the deterministic policy π_θ , the discounted sum of reward-to-go can be regarded as an estimate of the true state-value. Results show that the critic networks converge, but in most cases to an underestimated value. This is because the critic network is trained to fit the state-value function $V^\beta(s)$ of the stochastic exploration policy β rather than $V^{\pi_\theta}(s)$ of the deterministic policy π_θ . The underestimate bias vary in different tasks and when using different forms of policies, which is related to the local shape of the optima found by the RL agent. However, due to the objective function used in ZOAC, intuitively, the agent tend to find wide optima during training, which finally result in more robust policies.

Table 3. Max total average return within certain environmental steps (mean \pm std over 5 trials).

Environment	Inv.D.P.-v2	Hopper-v2	HalfCheetah-v2	Ant-v2	Human.Stand.-v2
Timesteps	1e6	2e6	2e6	2e7	2e7
ZOAC(Linear)	9359.93\pm0.01	3280.33\pm130.39	5201.63 \pm 270.75	4322.46.33\pm103.58	138229.85 \pm 26918.11
ZOAC(Neural)	9329.40 \pm 5.81	3359.90 \pm 146.40	5365.82\pm160.75	4233.75 \pm 46.64	190764.24\pm25894.95
ARS(Linear)	9359.85\pm0.06	2891.28 \pm 305.61	2967.98 \pm 889.42	3427.85 \pm 765.62	130137.60 \pm 1851.58
ES(Neural)	9155.73 \pm 404.25	1065.34 \pm 49.14	2349.11 \pm 444.77	3274.89 \pm 519.66	105216.15 \pm 12114.84
PPO(Neural)	9359.89\pm0.04	3178.60 \pm 270.09	5219.61 \pm 677.90	3796.13 \pm 754.78	153217.86 \pm 1603.05

Table 3 presents the max total average return with in certain environmental step threshold. ZOAC matches or outperforms baseline algorithms across tasks in the final performance, and variance over trials.

F. Details of the compact policies

Fully collected neural network can be presented as the connection of the following function in series:

$$y = f(W, b) = \phi(Wx + b) \quad (18)$$

where $x \in \mathbb{R}^n$ refers to the input vector, $y \in \mathbb{R}^m$ refers to the output vector, $W \in \mathbb{R}^{m \times n}$ refers to weight parameters, $b \in \mathbb{R}^m$ refers to bias parameters, and ϕ refers to element-wise nonlinear activation function.

Here we consider two different types of compact neural networks that compress the weight matrix W at each layer, to achieve a parameter number less than $m \times n$.

The first one is called Toeplitz network from (Choromanski et al., 2018). Toeplitz matrix is a kind of compact matrix with parameter sharing schemes, each element depends only on the difference between the row index and the column index. Hence, a Toeplitz matrix $T \in \mathbb{R}^{m \times n}$ has only $m + n - 1$ parameters.

The second one is called masked network from (Lenc et al., 2019; Song et al., 2021). It reduces the number of independent parameters by masking out redundant parameters (i.e., pruning). It setups another mask weight matrix $M \in \mathbb{R}^{m \times n}$. The near binary mask is then generated via $M' = \text{softmax}(M/\alpha)$. Softmax operation is applied element-wise and α is chosen to be 0.01. All parameters are concatenated and optimized using ZOAC. In order to encourage less parameters, we modify the advantage of each perturbed directions to be $A' = \beta A + (1 - \beta)(1 - \lambda)$, where A is the original normalized advantage function, λ is the usage of weight matrix parameters (i.e. effective edges), and $\beta \in [0, 1]$ is a weighting factor that anneals as training progresses.